Supplementary Discussion

Validation of the pyruvate/PEP ratio as a measure of PKM2 activity

A clear block in the flux from PEP to pyruvate was observed in shPKM cells where PEP accumulated faster, up to ~50-fold higher than in control cells, whereas the rate of pyruvate labelling was slower. In comparison to shPKM cells, the steady-state level of $^{13}C_3$-PEP in control cells was very low, and reached saturation after 5 minutes of U-^{13}C-glucose addition (Supplementary Fig 5). These results demonstrate that PKM1/2 (predominantly PKM2) activity in cells may be best represented as the ratio between 3-carbon labelled pyruvate ($^{13}C_3$-Pyr) (product) and ($^{13}C_3$-PEP) PEP (substrate) shortly after U-^{13}C-glucose addition. To verify this, a previously disclosed PKM2 activator, Cmpd1 (Supplementary Material and Methods), was tested to determine whether activating PKM2 would increase the $^{13}C_3$-Pyr /$^{13}C_3$-PEP ratio. Cmpd1 activated PKM2 with an AC_{50} of 0.51 µM and lowered the K_m for PEP 9.1-fold *in vitro* (Supplementary Fig. 6a-b). When HCT116 cells were incubated with Cmpd1 in U-^{13}C-glucose media, an increase in the ratio of labelled pyruvate to PEP was observed in shCntrl cells but not in shPKM cells (Supplementary Fig. 6c).

Interactions of serine with PKM2 in the amino acid binding pocket

Serine binding is facilitated by a re-orientation of the side chain of Arg106 which, in tandem with the side chain of Asn70, coordinates the carboxylic acid group of the serine (Supplementary Fig. 9c-d). The amino group of serine forms hydrogen bonds with the side chain of His464, the main chain carbonyl of Leu469 and a water molecule, which interacts with the main chain carbonyls of Tyr466 and His464. In addition, the side chain hydroxyl of the serine is hydrogen bonding with the main chain carbonyl of Leu469 and also with a water molecule that interacts with the main chain carbonyls of Gly468 and Asn44 (Supplementary Fig. 9c-d).

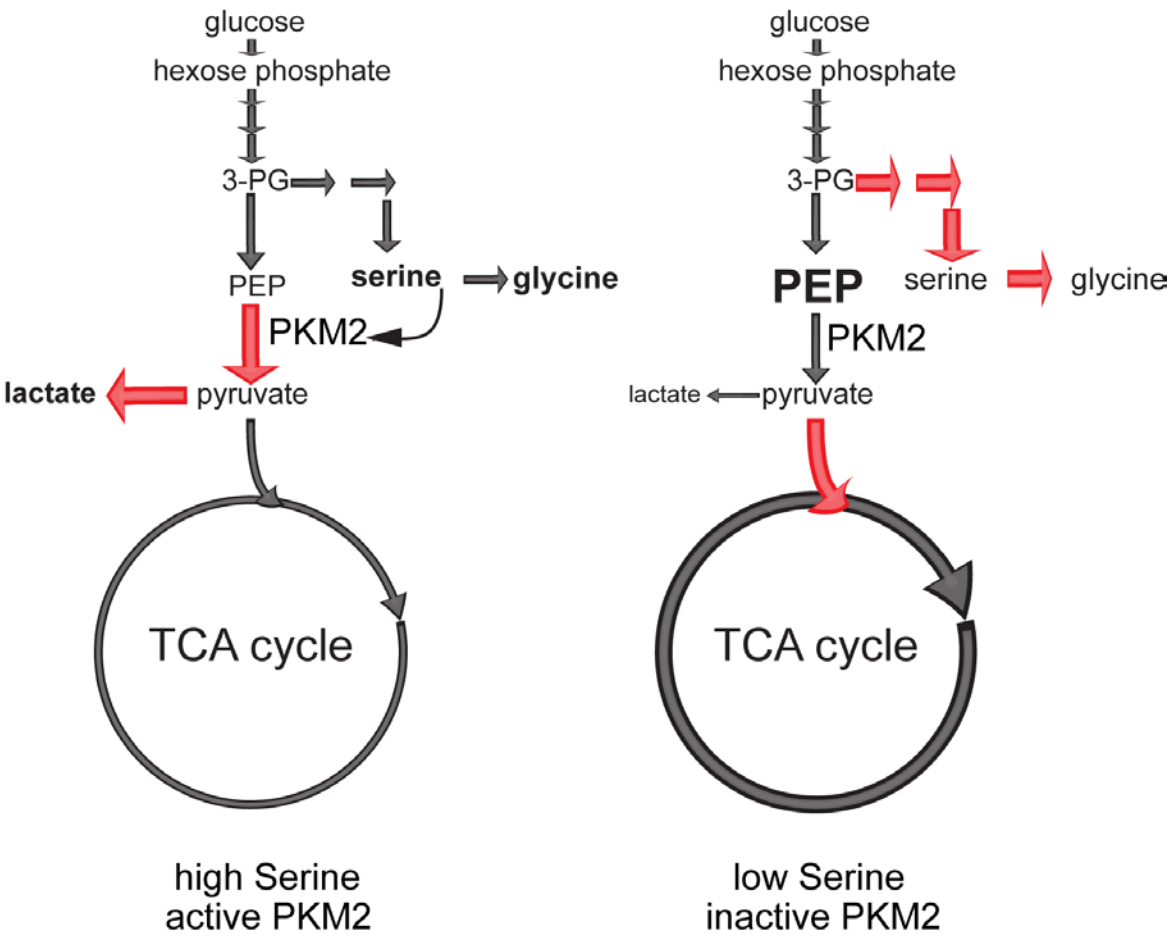

Supplementary Figure 1. **Serine activates PKM2 and regulates glycolysis.** Schematic representation of the major findings of the manuscript. When serine is abundant, PKM2 is fully active and glycolytic flux is increased. However, when the steady-state levels of serine drop below a critical point, PKM2 activity decreases and a fast shuttling of glucose-derived carbon to serine biosynthesis compensates for serine depletion. By regulating PKM2, serine also controls the fate of pyruvate in cells.

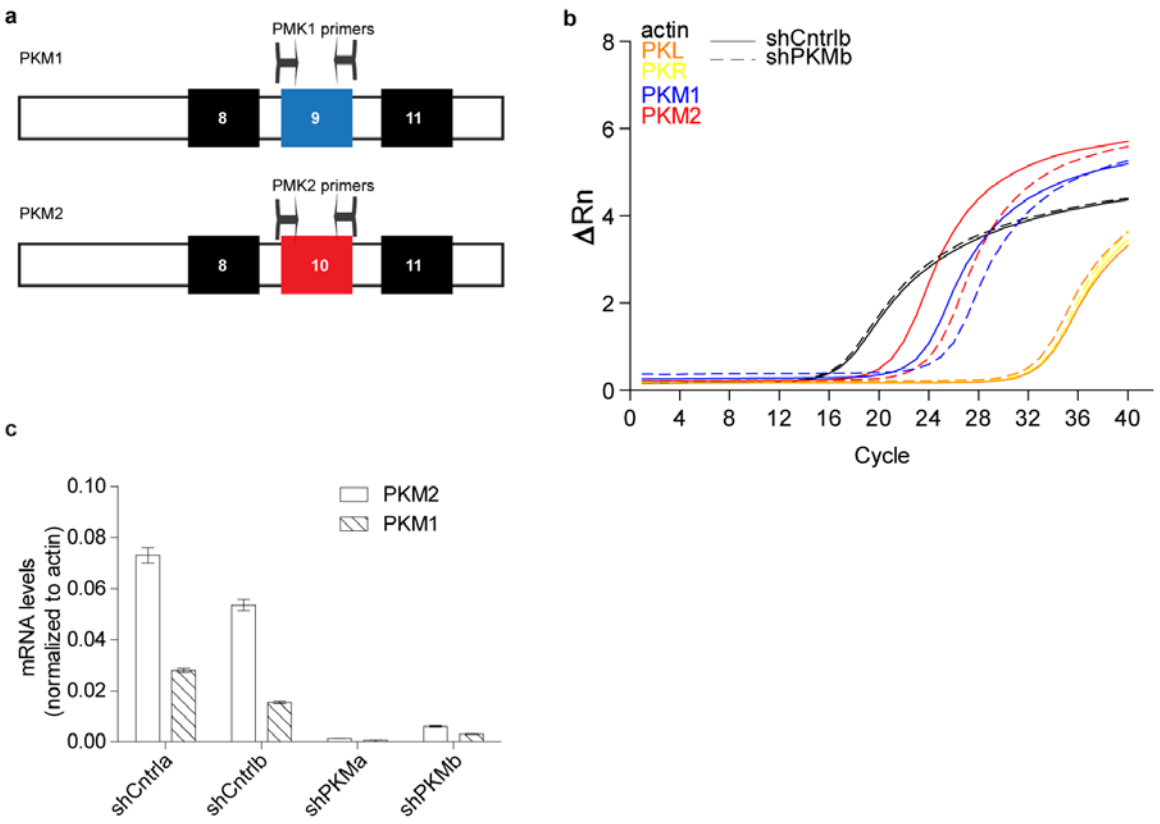

Supplementary Figure 2. **Expression levels of the different PK isoforms in HCT116 cells. a,** Schematic representation of primers used for the specific detection of PKM1 and PKM2 isoforms. For simplicity only exons 8 to 11 are indicated. **b,** Representative traces of a qPCR analysis of the indicated PK isoforms in control and PKM1/2-silenced cells. **c,** RNA expression levels of the PKM1 or PKM2 isoforms were measured by qPCR using specific primers for each isoform. HCT116 cells stably expressed either non-targeting control shRNA (shCntrl) or shRNA targeting both PKM isoforms (shPKM). shPKMa and shPKMb refer to two independent HCT116-derived cell lines, in which the expression of both the PKM1 and PKM2 isoforms was simultaneously and stably silenced using discrete shRNA pools, containing non-equivalent shRNAs.

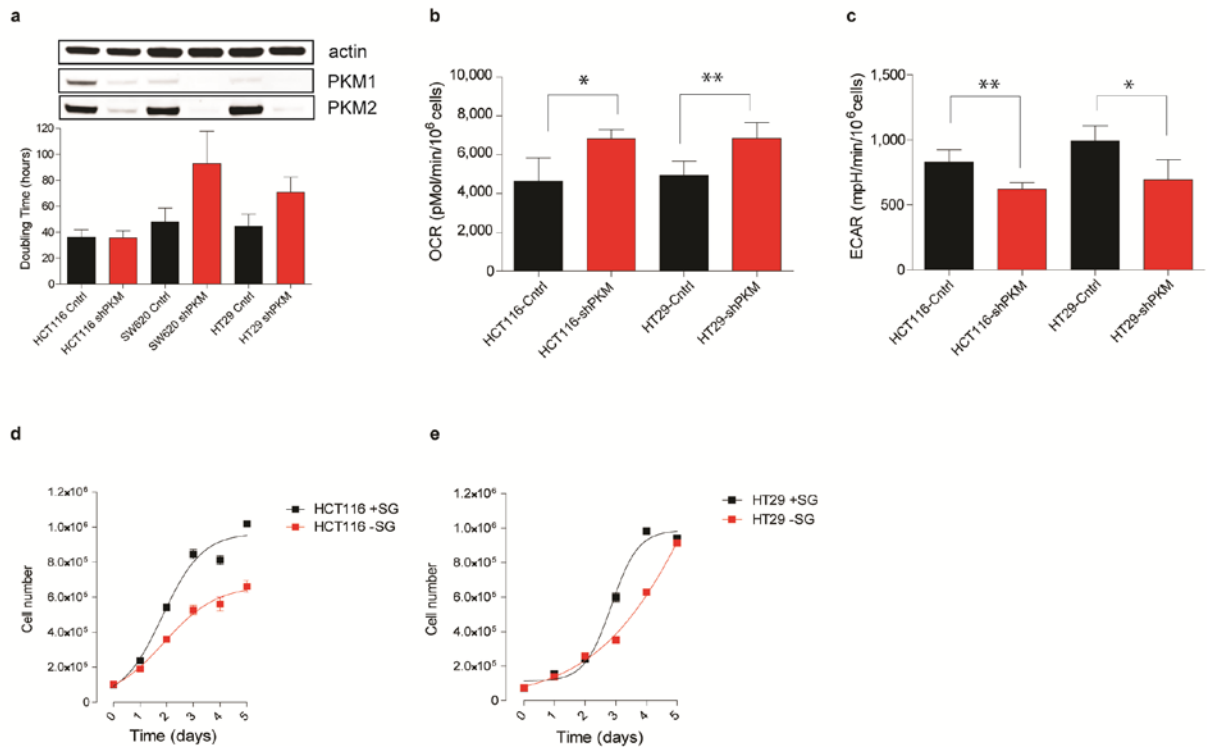

Supplementary Figure 3. **Effects of PKM1/2 silencing and serine/glycine deprivation. a,** Proliferation in HCT116, SW620 and HT29 cells infected with shCntrl or shPKM. Silencing of PKM increased doubling time in HT29 and SW620 cells but not in HCT116 cells. **b-c,** PKM1/2 silencing increased oxygen consumption rate (OCR) and decrease extracellular acidification rate (ECAR). **d-e,** Colon cancer cells are able to proliferate in the absence of serine and glycine although there is a decrease in the proliferation rate. * = P< 0.05, ** = P<0.01.

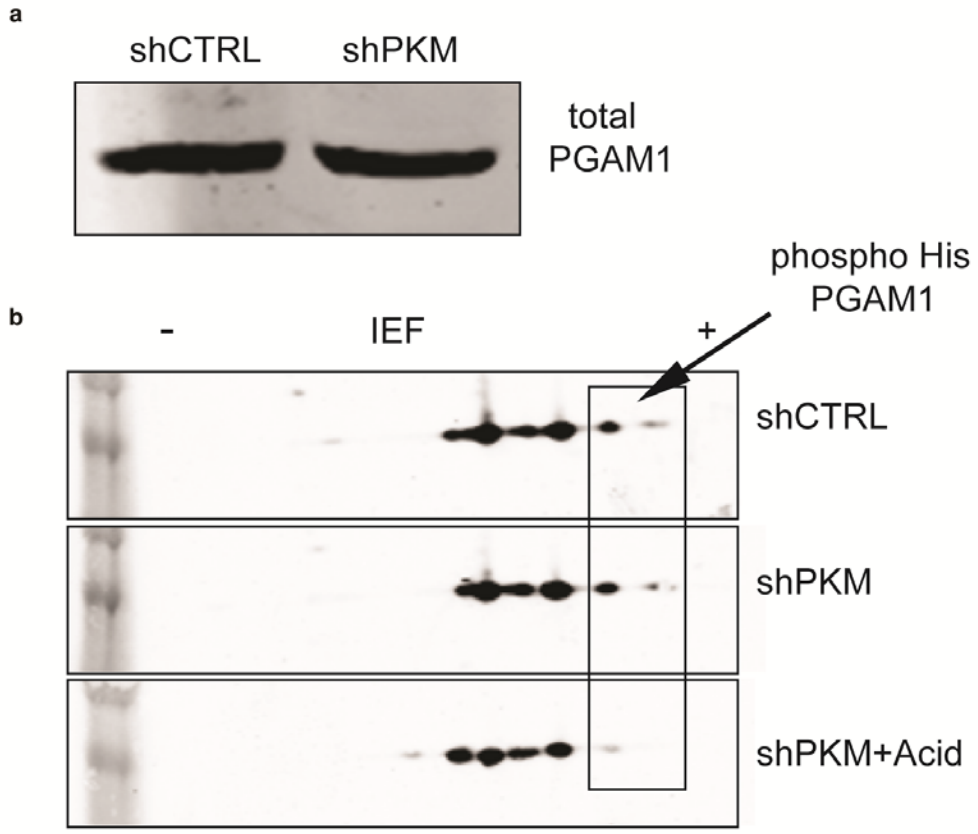

Supplementary Figure 4. **Effect of PKM1/2 silencing on Phosphoglycerate mutase (PGAM1) phosphorylation.** An alternative mechanism for converting PEP to pyruvate while phosphorylating PGAM1 on a histidine residue was suggested previously[9]. To test for this activity in PKM silenced cells we evaluated Histidine phosphorylation levels on PGAM1 by isoelectric focusing (IEF). **a,** PGAM1 protein levels in HCT116 cells shCntrl and shPKM were determined by Western blot. **b,** Cell lysates from HCT116 cells shCntrl or shPKM were subjected to 2D IEF and SDS-PAGE followed by Western blot for PGAM1. The most acidic forms in the 2D gel, shown in a box and marked with an arrow, correspond to phospho-histidine PGAM1. No changes in histidine phosphorylation levels were detected in HCT116 cells upon PKM1/2 silencing. Samples acidified to pH5 were used as negative controls.

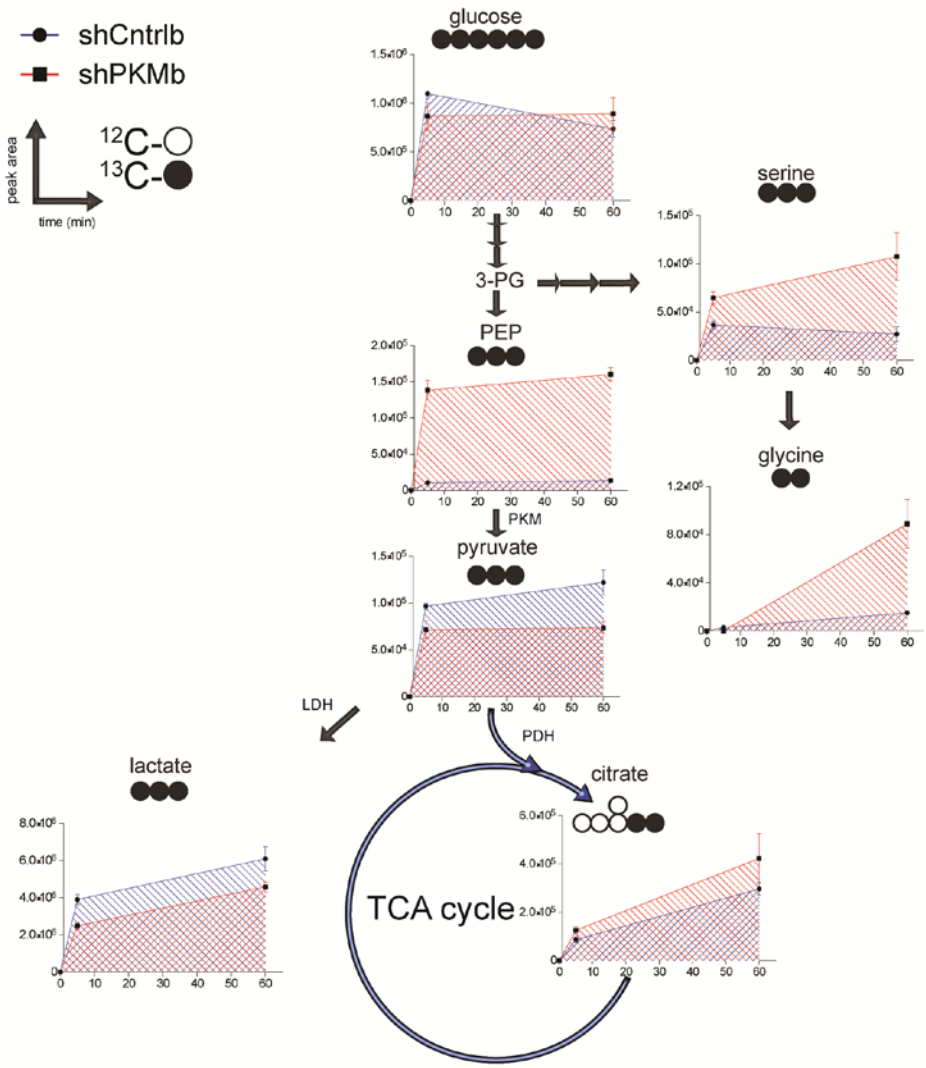

Supplementary Figure 5. **The effect of PKM1/2 silencing on glycolytic flux.** HCT116 cells were incubated with U-^{13}C-glucose and the abundance of the main glucose-derived isotopomer of the indicated metabolites was analysed at 5 and 60 minutes. The cumulative intensities of each labelled metabolite analysed in each cell line are presented in blue (shCntrl) or red (shPKM). The filled circles represent the ^{13}C-labelling of each metabolite. All metabolic quantifications were performed from 3 independent cultures and presented as mean ± s.e.m. 3-PG, 3-phosphoglycerate; PEP, phosphoenolpyruvate; PKM, pyruvate kinase; PDH, pyruvate dehydrogenase; LDH, lactate dehydrogenase; TCA, tricarboxylic acid.

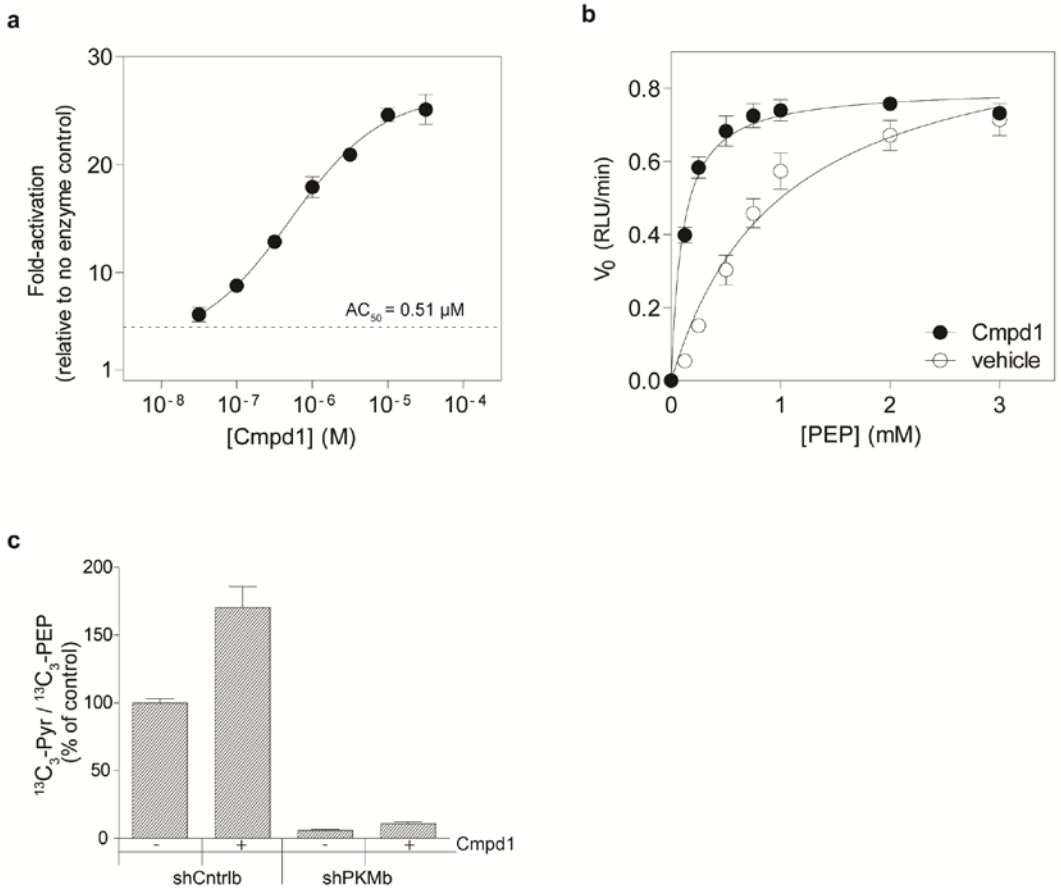

Supplementary Figure 6. ***In vitro*** **enzymatic and cellular activation of PKM2 by the specific PKM2 activator Cmpd1. a,** *In vitro* activity of recombinant human PKM2 was analysed in the presence of increasing concentrations of Cmpd1. Luminescence signal was normalised to no enzyme controls. The basal activity of PKM2 in the presence of vehicle control is indicated by a dotted line. **b,** The initial PKM2 reaction (V_0) was measured at different PEP concentrations in the presence of 30 µM Cmpd1. K_m values were determined as 1.0 mM and 0.11 mM in the presence of vehicle and Cmpd 1, respectively. **For a-b,** data are presented as mean ± s.e.m. of duplicate determinations. **c,** PK activity was measured in cells as the ratio between $^{13}C_3$-Pyr and $^{13}C_3$-PEP in the presence or absence of 20 µM Cmpd1 for 1 hour in shCntrl and shPKM cells. The indicated metabolites were measured by LC-MS. All the results are presented as mean ± s.e.m of 3 independent experiments.

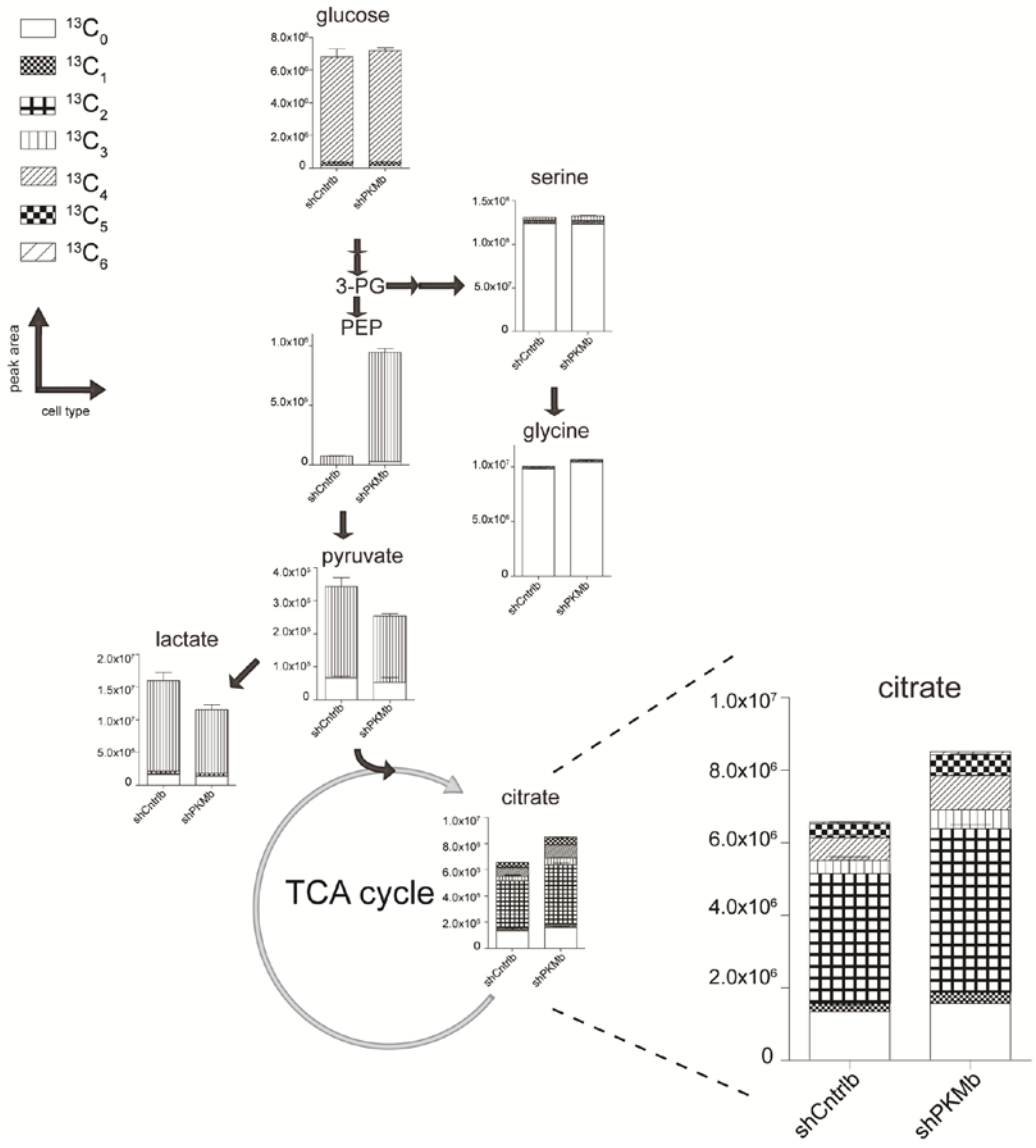

Supplementary Figure 7. **Isotopomer distribution of glycolytic intermediates in HCT116 cells.** The indicated cells were incubated with U-^{13}C-glucose for 4 hours and the isotopomer distribution of the studied metabolites was analysed by LC-MS. 3-PG, 3 phosphoglycerate; PEP, phosphoenolpyruvate. All the results are presented as mean ± s.e.m of 3 independent experiments.

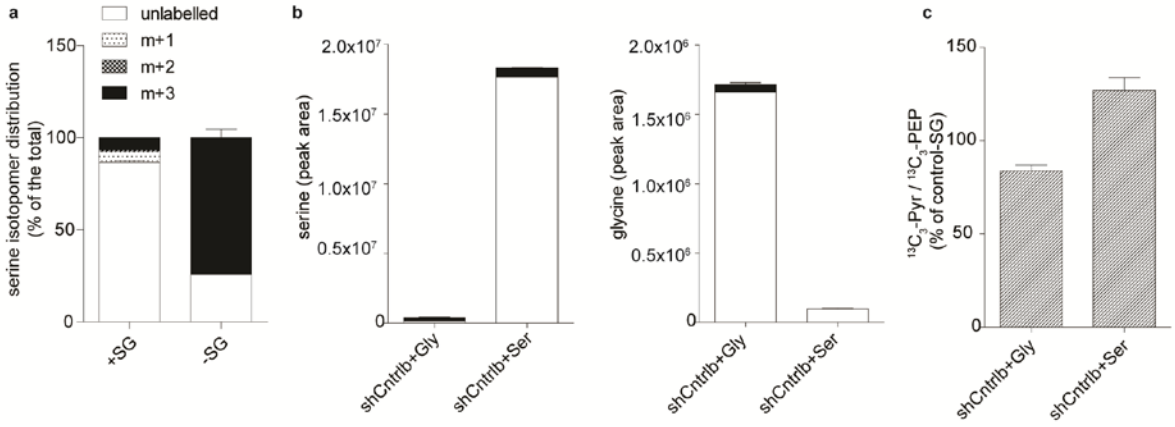

Supplementary Figure 8. **Serine but not glycine is an activator of PKM2 in cells. a,** isotopomer distribution of U-^{13}C-glucose-derived serine after 12 hours in the presence (+SG) or absence (-SG) of serine and glycine. **b,** The intracellular levels of serine or glycine were measured in cells starved of serine and glycine for 12 hours and then re-stimulated with either serine (+Ser) or glycine (+Gly) for 30 minutes. **c,** PK activation in cells by either serine (+Ser) or glycine (+Gly) alone was measured as the ratio between $^{13}C_3$-Pyr and $^{13}C_3$-PEP .Values are presented as percentage of PK activity in serine and glycine deprived cells. All the results are presented as mean ± s.e.m. of 3 independent experiments.

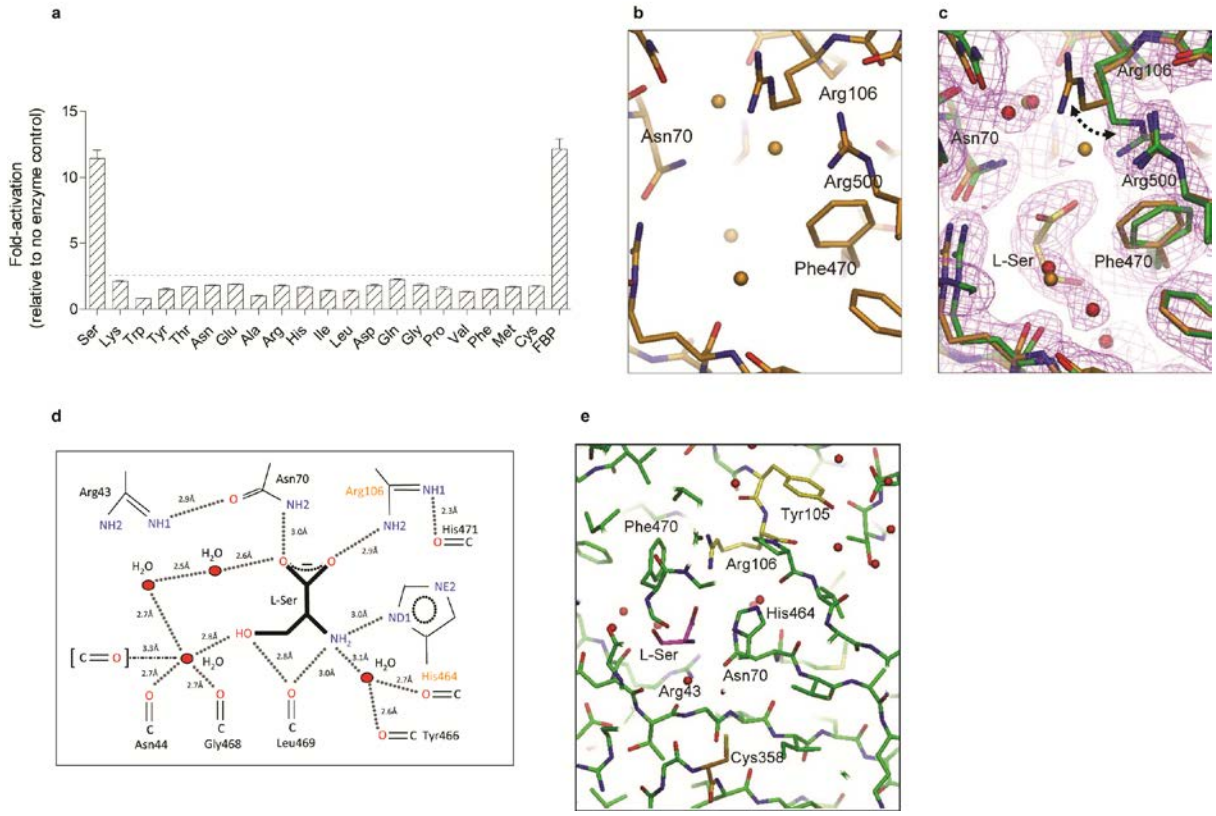

Supplementary Figure 9. **Detailed study of PKM2 and serine interactions. a,** PKM2 activity was measured *in vitro* in the presence of 10 mM of each of the 20 standard amino acids or 50 µM FBP. The signal was normalised to controls containing no enzyme. The basal activity of PKM2 in the presence of vehicle control is indicated by the dotted line. **b,** Structure of the vacant amino acid binding pocket in the reference structure 3BJF (hPKM2 co-crystallised with FBP, but not soaked with serine). **c,** Superposition of 3BJF (orange) and the final serine soaked (green) hPKM2 structures. Positive difference density is observed for serine and for the side chains of Arg106 and Phe470, which shift relative to the 3H6O PKM2 start model. Also shown is the final 2Fo-Fc map (purple: 1σ) for the serine-bound structure. **d,** Detailed schematic representation showing all L-ser interactions in the amino acid binding pocket of PKM2. **e,** Cys 358 and Tyr105 are situated in the vicinity of the amino acid binding pocket. The thiol group of Cys358 interacts with the carbonyl of His464, which forms key interactions with serine. The thiol of Cys358 is 7 Å from the serine's amine group. L-Ser in magenta, Cys 358 in orange, Tyr105 and Arg106 in yellow.

Supplementary Table 1 Data collection and refinement statistics (**Molecular replacement**)

	PKM2-Serine (PDB:4b2d)
Data collection	
Space group	$P2_1$
Cell dimensions	
a, *b*, *c* (Å)	80.61, 151.10, 91.79
α, β, γ (°)	90.00, 102.01, 90.00
Resolution (Å)	89.8-2.3(2.36-2.3) *
R_{sym} or R_{merge}	7.8(83.2)
$I/\sigma I$	11.5(1.6)
Completeness (%)	98(97.9)
Redundancy	3.7(3.5)
Refinement	
Resolution (Å)	2.3
No. reflections	93236
$R_{work/}$ R_{free}	17.9/22.7
No. atoms (non-hydrogen)	
Protein	15599
Ligand	(serine/FBP/Mg) 110
Water	908
B-factors	
Protein	62.2
Ligand	(serines) 39.5
Water	52.2
R.m.s deviations	
Bond lengths (Å)	0.011
Bond angles (º)	1.1

*Highest resolution shell is shown in parenthesis.
1 crystal used for data collection.
Additional crystallographic data statistics are provided in Supplementary Table 2

Supplementary Table 2 Crystallographic Data

Crystal

Unit cell (a,b,c)Å (α,β,γ)°	(80.61, 151.10, 91.79) (90.00, 102.01, 90.00)
Space group: $P2_1$ (#4)	
1 tetramer per asymmetric unit	
Collected at Diamond-I03	
Single crystal frozen at 100K	
Wavelength 0.9795Å	

Data collection

Resolution (Å)		89.8-2.3
% reject reflection		0.0
Rmerge (overall %)		7.8
Rmerge (outer shell % (2.36-2.3)Å)		83.2
Rmerge (inner shell % (80-10.2)Å)		1.5
% Completeness (80-2.3)Å		98.0
% Completeness (outer shell)		97.9
I/sigI (outer shell)		1.6
Average redundancy		3.7
Total number of unique reflections	93236	
Total number of non-hydrogen atoms in refinement	16617	

Effective resolution (2.36Å)

Resolution range (2.49-2.42)Å
Rmerge (%) 59.9
I/sigI 2.2
Completeness (%) 98

Resolution range (2.42-2.36)Å
Rmerge (%) 68.4
I/sigI 1.9
Completeness (%) 98

Refinement

Resolution (Å)	78.8-2.3
R factor (%)	17.9
R free (%)	22.7
RMS bond deviation (Å)	0.011
RMS angle deviation (°)	1.1
Ramachandran plots, labelled residues (dev. from mean)	57 (1.0)
Bad contacts: <2.6Å (dev. from mean)	13 (-0.7)
Peptide bond planarity (°) (dev, from mean)	5.6 (-0.1)
Overall G-factor (dev. from mean)	0.0 (1.7)

Serine in Amino Acid Binding Site Monomer A

Occupancy	.89
Difference density Z-score	0.20
Density correlation	0.99
Difference between ligand and site B factor ($Å^2$)	6.3

	Rmsd	Z-score	Max. Z-score	Outliers
Bonds(Å)	0.004	0.3	-0.5	
Angles(°)	0.5	0.3	-0.6	
Planes(Å)	0.0	0.4	0.4	
Torsions(°)	12.0	0.4	-0.4	

Serine in Amino Acid Binding Site Monomer B

Occupancy	1
Difference density Z-score	0.10
Density correlation	0.99
Difference between ligand and site B factor (Å^2)	2.2

	Rmsd	Z-score	Max. Z-score	Outliers
Bonds(Å)	0.005	0.4	0.6	
Angles(°)	1.1	0.8	1.7	
Planes(Å)	0.0	0.5	0.4	
Torsions(°)	18.0	0.6	0.8	

Serine in Amino Acid Binding Site Monomer C

Occupancy	.84
Difference density Z-score	0.50
Density correlation	0.98
Difference between ligand and site B factor (Å^2)	8.9

	Rmsd	Z-score	Max. Z-score	Outliers
Bonds(Å)	0.003	0.3	0.4	
Angles(°)	0.5	0.3	0.5	
Planes(Å)	0.0	0.3	-0.2	
Torsions(°)	26.0	0.9	1.1	

Serine in Amino Acid Binding Site Monomer D

Occupancy	.83
Difference density Z-score	0.40
Density correlation	0.98
Difference between ligand and site B factor (Å^2)	0.0

	Rmsd	Z-score	Max. Z-score	Outliers
Bonds(Å)	0.004	0.3	0.5	
Angles(°)	0.4	0.3	0.7	
Planes(Å)	0.0	0.9	0.8	
Torsions(°)	19.0	0.6	0.8	

Number of waters	908
B-factors (Å^2)	
Average B factor (all atoms, apart from waters)	62.2
Average B factor for main-chain atoms	60.0
Average B factor for side-chain atoms	64.9
Average B factor for waters	52.2
Average B factor from Wilson plot	45.7
Ligand B factor serine bound to monomer A	35.58
Protein B factor around serine site monomer A	41.9
Ligand B factor for serine bound to monomer B	42.24

Protein B factor around serine site monomer B	40
Ligand B factor for serine bound to monomer C	33.45
Protein B factor around serine site monomer C	42.4
Ligand B factor serine bound to momomer D	46.92
Protein B factor around serine site monomer D	46.9
Chi1-chi2 plots, labelled residues	15
Fo-Fc correlation factor	0.93
Estimated coordinate error (dpi)	-

	Overall	InnerShell	OuterShell
Low resolution limit (Å)	89.78	89.78	2.36
High resolution limit (Å)	2.30	10.29	2.30
Rmerge (%)	7.8	1.5	83.2
Rmerge in top intensity bin (%)	2.2	-	-
Rmeas (within I+/I-) (%)	9.2	1.8	97.9
Rmeas (all I+ & I-) (%)	9.2	1.8	97.9
Rpim (within I+/I-) (%)	4.8	0.9	51.1
Rpim (all I+ & I-) (%)	4.8	0.9	51.1
Fractional partial bias	0.000	0.000	0.000
Total number of observations	341189	3770	24336
Total number unique	93236	1043	6870
Mean((I)/sd(I))	11.5	45.6	1.6
Completeness (%)	98.0	94.9	97.9
Multiplicity	3.7	3.6	3.5
Anomalous completeness (%)	91.2	90.4	90.5
Anomalous multiplicity	1.9	1.9	1.8
DelAnom correlation between half-sets	-0.058	0.033	-0.010
Mid-Slope of Anom Normal Probability	0.940	-	-

Outlier rejection and statistics assume that there is no anomalous scattering

$R_{merge} = \Sigma\Sigma_j|I_{hj} - \langle I_h \rangle|/\Sigma\Sigma_j I_{hj}$
$R_{meas} = \Sigma\sqrt{(n/(n-1))}\ \Sigma_j|I_{hj} - \langle I_h \rangle|/\Sigma\Sigma_j I_{hj}$ multiplicity-weighted R_{merge}
$R_{p.i.m} = \Sigma\sqrt{(1/(n-1))}\ \Sigma_j|I_{hj} - \langle I_h \rangle|/\Sigma\Sigma_j I_{hj}$ precision indicating R_{merge}
$R = \Sigma_h\{|F_o|-|F_c|\}/\Sigma_h|F_o|$ Where F_o and F_c are the observed and calculated structure factor amplitudes respectively
R_f = as R but for an independent 5% test set of reflections excluded from the modelling and refinement process

(See references 31-34 in the Supplementary Materials and Methods)